Energy Management in Microgrids with Battery Swap Stations and Var Compensators

A. Rezaee Jordehi[a,1] , Mohammad Sadegh Javadi [2] , João P. S. Catalão [2,3]

[a]*Department of Electrical Engineering, Rasht Branch, Islamic Azad University, Rasht, Iran*

[2] *INESC TEC, Porto, Portugal*

[3]*Faculty of Engineering of the University of Porto, Porto, Portugal*

Abstract-The scarcity and price volatility of fossil fuels as well as environmental concerns has motivated the replacement of fossil fuel-powered vehicles by electric vehicles (EVs). Long charging time in battery charging stations is a serious barrier for large-scale adoption of EVs, so battery swap stations (BSSs) were developed wherein the near-empty batteries are exchanged with fully charged batteries and EV refilling is done in only a couple of minutes. Nowadays, BSSs are typically connected to a microgrid (MG) in their neighborhood. In this research, the optimal scheduling of MG resources and BSS is done for a grid-connected MG with dispatchable, photovoltaic and wind distributed generation (DG) units and operation cost of MG is minimised. It is assumed that the BSS services Tesla 3 EVs with 75 kWh batteries and a driving range of 496 km. A var compensator (VC) is connected to the MG that can purchase reactive power from var compensator. AC optimal power flow is done for the MG, while all network constraints, power loss and reactive power dispatch are taken into account and the cost of provision of reactive power is included in the operation cost of the MG. Generalized reduced-gradient (GRG) algorithm is used for the optimisation process. The effects of VC, optimal BSS scheduling and reactive power costs on active/reactive power dispatch and MG operation cost are duly investigated.

Keywords: battery swap stations; reactive power cost; microgrids; energy management system; electric vehicles.

[1]Corresponding author at: Rasht Branch, Islamic Azad University, Rasht, Iran.
E-mail address: ahmadrezaeejordehi@gmail.com.

Nomenclature

Indices

i, k Indices of buses

j Index of dispatchable DGs

pv Index of PV units

w Index of wind units

vc Index of var compensator units

bss Index of BSS units

t Index of time

Sets

S Set of buses

GR Set of buses with point of common coupling (PCC)

R Set of buses excluding the bus with PCC

U Set of buses with var compensator

B_i Set of buses connected to bus i

E Set of buses with BSS

J Set of dispatchable DGs

J_i Set of dispatchable DGs connected to bus i

BR Set of branches

BR_i Set of branches connected to bus i

F Set of time periods excluding the first time period

H Set of time periods excluding the last time period

O Set including the first time period

Parameters

a, b, c Coefficients of bid function of dispatchable DGs for real power

d Bid of reactive power of dispatchable DGs

RU Maximum ramp-up rate of dispatchable DGs

RD Maximum ramp-down rate of dispatchable DGs

P_{min} Minimum active power of dispatchable DGs

P_{max} Maximum active power of dispatchable DGs

Q_{min} Minimum reactive power of dispatchable DGs

Q_{max} Maximum reactive power of dispatchable DGs

α_i Availability of wind power at bus i

β_i Availability of PV unit at bus i

δ_i Availability of BSS at bus i

$BSScap_i$ Capacity of BSS at bus i

$Q_{vc,i,max}$ Maximum reactive power of VC at bus i

$Q_{vc,i,min}$ Minimum reactive power of VC at bus i

π_t Bid of VC at time t

$W_{i,t}$ Wind power at bus i and time t

$PV_{i,t}$ PV power at bus i and time t

ρ_t Market price at point of common coupling (PCC) at time t

$P_{grid,max}$ Maximum capacity of the link between MG and grid

$PD_{i,t}$ Active power demand at bus i and time t

$QD_{i,t}$ Reactive power demand at bus i and time t

$R_{i,k}$ Resistance of branch between bus i and bus k

$X_{i,k}$ Reactance of branch between bus i and bus k

$Z_{i,k}$ Magnitude of series impedance phasor of branch between bus i and bus k

$\theta_{i,k}$ Angle of phasor of series impedance of branch between bus i and bus k

$B_{i,k}$ Susceptance of branch between bus i and bus k

$Plim_{i,k}$ Real power flow limit of branch between bus i and bus k

$Qlim_{i,k}$ Reactive power flow limit of branch between bus i and bus k

V_{min} Minimum allowable voltage magnitude of buses

V_{max} Maximum allowable voltage magnitude of buses

$E_{bss,,i,ini}$ Initial energy level of BSS at bus i

$E_{bss,,i,min}$ Minimum allowed energy level of BSS at bus i

$P_{bss,i,max}$ Maximum exchangeable power between BSS at bus i and MG

$Pshed_{i,max}$ Maximum real power at bus i that may be shed

$VOLL_t$ Value of lost load at time t

Variables

$Pf_{i,k}$ Real power flow of branch between bus i and bus k

$Qf_{i,k}$ Reactive power flow of branch between bus i and bus k

$I_{i,k}$ Phasor of current of branch between bus i and bus k

$S_{i,k}$ Apparent power of branch between bus i and bus k

$P_{j,t}$ Real power of jth dispatchable DG at time t

$Q_{j,t}$ Reactive power of jth dispatchable DG at time t

$P_{grid,t}$ Power exchange between MG and grid

$Pshed_{i,t}$ Shed real power at bus i and time t

$Q_{vc,i,t}$ Reactive power of VC at bus i and time t

$P_{bss,i,t}$ BSS power at bus i and time t

$E_{bss,i,t}$ BSS energy level at bus i and time t

C_P Active power cost of MG

C_Q Reactive power cost of MG

C Daily operation cost of MG

V Voltage magnitude

Va Voltage angle

Dual variables

LMP Locational marginal price of active power

LMQ Locational marginal price of reactive power

1. Introduction

The scarcity and price volatility of fossil fuels along with serious environmental concerns motivated transportation electrification and the fossil fuel-powered vehicles are being replaced by electric vehicles. The penetration of EVs in vehicle markets is increasing and incentives are offered to encourage the usage of EVs instead of conventional vehicles (Mahoor et al., 2019).

Thanks to offered incentives and the advances in battery technologies, it is envisioned that the share of EVs in the global vehicle market reaches 22% by 2030 and 35% by 2040 (Mahoor et al., 2019). Despite their benefits (Han et al., 2010; Islam et al., 2019), the challenge in charging is a barrier for larger adoption of EVs and of paramount importance. EV chargers are classified into three levels. The level 1 and level 2 chargers are slow chargers respectively with maximum power 1.92 kW and 19.2 kW and are commonly used at households and workplaces where the charging time is not much important (Turksoy et al., 2019; Xu et al., 2020). The maximum power in level 3 chargers is higher than 19.2 kW and they offer faster charging than level 1 and level 2 chargers and are commonly used at battery charging stations (BCSs) (Xu et al., 2020). The charging time in BCSs depends on charging power and EV battery capacity and takes a considerable time, while EV owners expect to refill as short as conventional fossil-powered vehicles. Long charging time of EVs and the range anxiety defined as the fear of EV drivers of running out the electricity before reaching the destination or next BCS are big barriers for higher popularity of EVs (Xu et al., 2020).

In order to mitigate the challenges of charging EVs with BCSs, battery swap stations (BSSs) were developed wherein the near-empty batteries are exchanged with fully charged batteries. Refilling in BSS takes only a few minutes; Tesla in 2013 showed that the battery swap of its model S takes only 90 seconds . In this way, batteries of EVs are leased to EV owners, so the battery price is deducted from EV price and the sticker price of EV is significantly reduced as battery price is a considerable portion of EV price (Mahoor et al., 2019). Even in recent years, for ease of EV charging, some mobile BSSs have been developed . For efficient usage of battery swapping, high-range batteries with high energy density must be used (Mahoor et al., 2019). Commonly, in BSSs there exist chargers with different charging speeds.

BSSs are connected to power grids. Using BSSs offers benefits for all involved stakeholders including power grid, BSS owner and EV owners. Some of those benefits are listed out below.

- Since the battery is leased to EV owners, they pay less to buy EV.
- The range anxiety of EV owners is decreased and they enjoy fast charging.

- The battery to grid (B2G) capability of BSSs may function as a spinning reserve for power grid.
- Through their B2G capability, BSSs may take part in energy and reserve markets and increase their profit.
- BSSs function as responsive loads for power grids. Power grids may decrease their operation cost using such responsive loads.
- BSSs decrease the burden of uncontrolled EV charging on power grids.
- Since the batteries are stocked in BSS, it may charge the batteries at low-price times and decrease its operation cost.

As BSSs are connected to grids/MGs, the operation of grids/MGs with BSS is an important issue (Meral and Çelík, 2019). In this regard, we are dealing with three types of stakeholders; grid owner, BSS owner and EV owners. In literature, the optimal operation is either done from the perspective of BSS owner or perspective of grid/MG or in some cases, it is done considering both BSS and grid/MG benefits.

In (Mahoor et al., 2019), in a BSS, connected to a power grid, charging/discharging schedule of batteries is determined in a way that BSS operation cost including the cost of power purchased from grid and battery degradation cost is minimised. The uncertainties of BSS demand and market price have been dealt with robust optimisation. The operational constraints such as minimum/maximum state of charge, minimum/maximum charging and discharging power and minimum charging/discharging time of batteries as well as exchange limit with grid have been considered. Benders decomposition has been used for solving the proposed robust model, wherein the master problem determines decision variables and the sub-problem determines the worst case of BSS. The results have been achieved for different Tesla EV models in order to find the effect of battery type on BSS operation cost. The effect of the number of batteries inside BSS on BSS operation cost has also been investigated. As expected, with increasing the number of batteries inside BSS, its operation cost decreases.

In (Li et al., 2018), a bi-level optimisation with chance constraints has been used for optimal operation of an isolated MG including BSS. The first level minimises the operation cost of the MG including operation cost of

DGs and reserve cost and the second level minimises the operation cost of BSS. Both MG and BSS must keep their supply-demand balance. MG has set a real-time tariff for BSS and the arrival time of EVs to BSS has been modeled as the Poisson probability density function .The operation cost of BSS is determined by subtracting its revenues, including B2G revenue and reserve revenue and its costs including the cost of power purchased from MG and battery degradation costs. Jaya optimisation algorithm and benders decomposition have been respectively used for solving the first and second level problems.

In (Wu et al., 2017), genetic algorithm (GA) and differential evolution (DE) with variable population size have been used for optimal operation of BSSs, while the objective includes stock level and degradation of batteries as well as charging cost. The population is varied depending on the average difference between the best individual and other individuals. Charging/discharging schedule and charging/discharging power of batteries are determined by the proposed optimisation algorithms. In (Amiri et al., 2018), four BSSs have been connected to different buses of a power system and optimal BSS for charging each vehicle and also optimal order of charging depleted batteries are determined. Non-dominated sorting GA (NGGA-II) is used for optimisation and minimises charging cost of BSSs, while the power and voltage constraints of the power system are met. In (Wang et al., 2019), BSS is connected to an MG, AC optimal power flow is used for optimal dispatch of MG and a mixed-integer linear programming (MILP) formulation has been formed to determine the charging schedule of batteries in BSS. The objective function for BSS includes its charging cost and battery degradation costs.

In (Moaidi and Golkar, 2019), operation problem of a BSS connected to a power system is formulated as a mixed-integer nonlinear programming (MINLP) and is solved with LINDO solver in general algebraic modeling system (GAMS). Optimal charging schedule of batteries is determined, while the start, duration and end of EVs' trip are modeled as probability density functions and Monte Carlo simulation (MCS) is used for dealing with uncertainties. It is assumed that when the state of charge of an EV falls below a limit, it goes to

BSS. The objective of the optimisation problem is to minimise BSS operation cost, namely the cost of power purchased from grid minus the revenue from the battery swapping with EVs.

In (Liang and Zhang, 2018), optimal BSS charging strategy is determined so that the aggregate benefit of all stakeholders including BSS, power grid and EV owners are maximised. In (Yan et al., 2019), energy management of a MG with BSS has been done while BSS serves as an energy storage system and reserve for MG. In (Gao et al., 2012), particle swarm optimisation (PSO) has been used for optimal operation of a MG with wind generators and BSS, while BSS serves as an energy storage system for MG and mitigates the volatility of wind generator(s).

With review of the literature, the following issues must be pointed out.

- In most cases, reactive power dispatch has not been considered.
- The cost of reactive power has not been considered in operation of grid/MG.
- The effect of reactive power resources on the MG operation has not been investigated.

Considering the aforementioned issues, in this research optimal power flow of MGs with BSS is done while both MG and BSS are owned by the same entity. A var compensator (VC) is connected to the MG and MG can purchase reactive power from VC. Through reactive power support, VCs may enhance voltage stability of MGs (Javadi et al., 2017).

The contributions of this research are listed out as below.

- Optimal power flow is considered for a grid-connected MG with its own BSS, taking into account all network constraints and reactive power dispatch.
- A VC is connected to the MG and MG can purchase reactive power from VC.
- The cost of reactive power provision is included in the operation cost of the MG.
- The effects of VC and reactive power cost on the operation cost of the MG are investigated.

2. Problem Formulation

The objective is to minimise the operation cost of MG over the scheduling horizon. The operation cost of MG includes the cost of active and reactive power provision, respectively represented by (1) and (2). The total operation cost is given by (3). The cost of active power, represented by (1) includes three different terms; cost of purchasing real power from dispatchable DGs, cost of purchasing real power from grid and cost of load shedding. For each time, if power is imported from grid, $P_{grid,t}$ would be positive and represents a cost; on the other hand, if power is exported to the grid, $P_{grid,t}$ would be negative and represents a benefit for MG rather than a cost (Jordehi, 2020a, b). The reactive power cost, represented by (2), includes the cost of purchasing reactive power from dispatchable DGs and VCs.

$$C_P = \sum_t \sum_j a_j \left(P_{j,t}\right)^2 + b_j P_{j,t} + c_j + \sum_t P_{grid,t} \cdot \rho_t + \sum_i \sum_t Pshed_{i,t} \cdot VOLL_t \quad (1)$$

$$C_Q = \sum_t \sum_j d_j Q_{j,t} + \sum_i \sum_t Q_{VC,i,t} \cdot \pi_t \quad (2)$$

$$C = C_P + C_P \quad (3)$$

Power flow equations are represented as (4)-(10). Real power balance equations are imposed as (4) and (5). The set of equations, represented by (4), is imposed for all buses except for the bus with point of common coupling (PCC) and (5) represents real power balance equations for bus with PCC. According to (4), at each bus and at each time, sum of real power of dispatchable DGs connected to that bus, shed power, PV power and wind power must be equal to sum of real power demand at that bus, BSS power at that bus and real power of branches connected to that bus. For buses with BSS, δ_i is one and for other buses, it is zero.

As (6), at each bus and at each time, sum of reactive power of dispatchable DGs connected to that bus and reactive power of VC must be equal to sum of reactive power demand of the bus and reactive power of branches connected to the bus.

$$\sum_{j\epsilon J_i} P_{j,t} + Pshed_{i,t} + PV_{i,t} + W_{i,t} - PD_{i,t} - \delta_i P_{bss,i,t} = \sum_{k\epsilon B_i} Pf_{i,k,t} \quad \forall i\epsilon R, \forall t \tag{4}$$

$$\sum_{j\epsilon J_i} P_{j,t} + Pshed_{i,t} + PV_{i,t} + W_{i,t} - PD_{i,t} - \delta_i P_{bss,i,t} + P_{grid,t} = \sum_{k\epsilon B_i} Pf_{i,k}, t \quad \forall i\epsilon GR, \forall t \tag{5}$$

$$\sum_{j\epsilon J_i} Q_{j,t} + Q_{vc,i,t} - QD_{i,t} = \sum_{k\epsilon B_i} Qf_{i,k,t} \quad \forall i, \forall t \tag{6}$$

$$\boldsymbol{I}_{i,k,t} = \frac{V_{i,t}\angle Va_{i,t} - V_{k,t}\angle Va_{k,t}}{Z_{i,k}\angle\theta_{i,k}} + \frac{B_{i,k}}{2}\angle\left(\frac{\pi}{2} + Va_{i,t}\right) \qquad \forall i, \forall k \in B_i, \forall t \tag{7}$$

$$\boldsymbol{S}_{i,k,t} = V_{i,t}\angle Va_{i,t} \,.\, \boldsymbol{I}^*_{i,k,t} \quad \forall i, \forall k \in B_i, \forall t \tag{8}$$

$$Pf_{i,k,t} = \frac{V_{i,t}^2 \cos(\theta_{i,k})}{Z_{i,k}} - \frac{V_{i,t}.V_{k,t}}{Z_{i,k}} \cos(Va_{i,t} - Va_{k,t} + \theta_{i,k}) \qquad \forall i, \forall k \in B_i, \forall t \tag{9}$$

$$Qf_{i,k,t} = \frac{V_{i,t}^2 \sin(\theta_{i,k})}{Z_{i,k}} - \frac{V_{i,t}.V_{k,t}}{Z_{i,k}} \sin(Va_{i,t} - Va_{k,t} + \theta_{i,k}) - \frac{B_{i,k}}{2} V_{i,t}^2 \qquad \forall i, \forall k \in B_i, \forall t \tag{10}$$

For dispatchable DGs in MG, ramp rate limits are imposed as (11) and (12). These constraints do not allow rapid changes in power of DGs and preclude severe mechanical stress on rotor. The constraints on real and reactive power of dispatchable DGs are imposed as (13)-(14).

$$P_{j,t} - P_{j,(t-1)} \leq RU_j \quad \forall g, \forall t \in F \tag{11}$$

$$P_{j,(t-1)} - P_{j,t} \leq RD_j \quad \forall g, \forall t \in H \tag{12}$$

$$P_{min,j} \leq P_{j,t} \leq P_{max,j} \qquad \forall j, \forall t \tag{13}$$

$$Q_{min,j} \leq Q_{j,t} \leq Q_{max,j} \qquad \forall j, \forall t \tag{14}$$

The operation of BSS is subject to constraints (15)-(19). Equations (15) are imposed to ensure that all empty batteries arrived to each BSS are fully charged at the end of the scheduling horizon. Power of BSS may be

positive (charging mode), negative (discharging mode) or zero (idle mode). According to (16), the energy level of each BSS at each time period is equal to the summation of its charging/discharging power at that time and its energy level at previous time. According to the set of equations represented by (17), energy level of each BSS at the first time period is calculated by summation of its charging/discharging power at that time and its initial energy level. BSS operation is also subject to limits on its energy level and charging/discharging power, as represented by (18) and (19). In this research, charging and discharging processes of batteries have been assumed lossless.

$$\sum_t P_{bss,i,t}\,\delta_i = BSScap_i \quad \forall i \in E \tag{15}$$

$$E_{bss,i,t} = E_{bss,i,(t-1)} + P_{bss,i,t} \quad \forall i \in E, \forall t \in F \tag{16}$$

$$E_{bss,i,t} = E_{bss,,i,ini} + P_{bss,i,t} \quad \forall i \in E, \forall t \in O \tag{17}$$

$$E_{bss,i,t} \geq E_{bss,i,min} \quad \forall i \in E \tag{18}$$

$$-P_{bss,i,max} \leq P_{bss,i,t} \leq P_{bss,i,max} \qquad \forall i \in E, \forall t \tag{19}$$

The MG is also subject to constraints for real power of branches, reactive power of branches and voltage of buses, respectively represented by (20)-(22).

$$-Plim_{i,k} \leq Pf_{i,k,t} \leq Plim_{i,k} \qquad \forall i, \forall k \in B_i, \forall t \tag{20}$$

$$-Qlim_{i,k} \leq Qf_{i,k,t} \leq Qlim_{i,k} \qquad \forall i, \forall k \in B_i, \forall t \tag{21}$$

$$V_{min,i} \leq V_{i,t} \leq V_{max,i} \qquad \forall i, \forall t \tag{22}$$

As (23), power exchange with grid is limited by power flow limit of the link connecting MG and grid. As per (24), the shed power at each bus and each time is limited by an upper limit, prespecified by the agreement between demand and MG operator. Finally, the operation of VC is subject to the constraints on its reactive power, as represented by (25).

$$-P_{grid,max} \leq P_{grid,t} \leq P_{grid,max} \qquad \forall t \tag{23}$$

$$0 \leq Pshed_{i,t} \leq Pshed_{i,max} \qquad \forall i, \forall t \tag{24}$$

$$Q_{vc,i,min} \leq Q_{vc,i,t} \leq Q_{vc,i,\max} \quad \forall i \in U, \forall t \tag{25}$$

3. Proposed Optimisation Algorithm

CONOPT is a generalized reduced-gradient (GRG) algorithm and considered as a powerful and fast optimisation algorithm for highly nonlinear models, in particular the formidable models wherein feasibility is difficult to achieve (Drud, 1994). Assume an optimisation problem with m decision variables and n equality constraints with the following form:

$$Min\, f(X)$$

$$g(X) = b \tag{26}$$

$$LO \leq X \leq UP$$

The steps of GRG algorithm are briefly described as below (Drud, 1994). To find more details of CONOPT, refer to (Drud, 1985; Drud, 1994).

1. The algorithm is initialised with a feasible solution.
2. The Jacobian of the constraints is computed.
3. The variables are categorised into n basic variables and $m - n$ non-basic variables.
4. Multipliers are calculated.
5. Reduced gradient is calculated.
6. Algorithm terminates here if the current point meets Kuhn-Tucker conditions, otherwise it is continued.
7. Non-basic variables are categorised into super-basic variables and fixed non-basic variables.
8. Based on super-basic component of reduced gradient and an estimate of the Hessian of the reduced objective, a search direction is found for super-basic variables.
9. A uni-dimensional search is done along the calculated direction and a pseudo-Newton method is used to adjust basic variables.
10. The algorithm is terminated if termination criterion is met, otherwise it goes to step 2. Tucker conditions

4. Results and analysis

A grid-connected MG with 33 buses, 32 branches, 4 dispatchable DGs, 2 wind DGs, 2 PV DGs, 1 VC and 1 BSS is used as case study. The single line diagram of the MG can be seen as Fig.1 and its bus and branch data

of can be found in (Shirmohammadi and Hong, 1989). The peak active and reactive power demand of the MG excluding BSS are respectively 3715 kW and 2300 kVAr. Dispatchable DGs are located at buses 2, 11, 15 and 27 and their data can be found in Table 1. Two 500 kW and 350 kW wind turbines are respectively available at buses 12 and 17. Two 400 kW and 500 kW PV units are respectively available at buses 18 and 24. A 500 kVAr VC is connected to bus 32 and a BSS is available at bus 33. It is assumed that the BSS services Tesla 3 EVs with 75 kWh batteries, driving range of 496 km and energy consumption of 15 kWh/100 km . It is also assumed that at a 24-h horizon, 200 Tesla 3 EVs arrive at BSS to exchange their empty batteries with fully-charged batteries. Table 2 contains time factors of demand, PV and wind generation and market price over the horizon of a day. These time factors show how demand, PV and wind generation and market price vary at different hours of the day. As an example, for 500 kW wind DG at bus 12, time factor of 0.07867 at hour 1 means that this wind DG produces 500×0.07867=39.335 kW at this hour. Due to the effect of variations of demand, PV and wind power and market price on optimal dispatch of MG, they have been illustrated as Fig.2 and Fig.3. The capacity of the link between MG and grid is 2 MW, bid of VC is 0.046 $/kVAr, value of loss of load (VOLL) is 100 $/kWh, initial energy level of BSS is zero and maximum power flow between BSS and MG is 2 MW. The minimum and maximum voltage levels of buses are respectively assumed as 0.90 and 1.10 pu. Base apparent power and voltage are respectively 1 MVA and 12.66 kV.

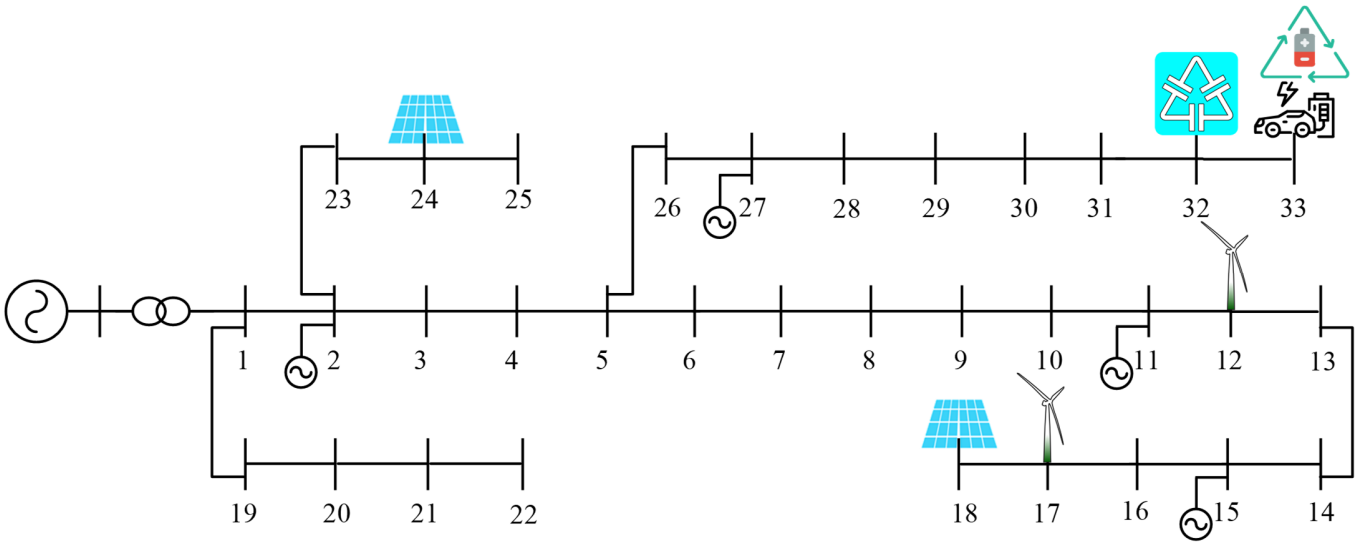

Fig.1. Single line diagram of the studied MG

Table 1. Data of dispatchable DGs

Bus number	P_{min} (kW)	P_{max} (kW)	Q_{min} (kVAr)	Q_{max} (kVAr)	a($/kWh)	b ($/kWh)	c($/kWh)	d($/kWh)	RU (kW)	RD (kW)
2	300	2500	0	1000	0	0.154	0	0.040	500	500

11	300	1000	0	1000	0	0.157	0	0.044	400	400
15	200	1000	0	500	0	0.218	0	0.051	300	300
27	200	1000	0	300	0	0.194	0	0048	300	300

Table 2. Time factors of demand, PV and wind generation and market price at point of common coupling (PCC)

Hour	Demand (Khodaei, 2013)	PV (Rezaee Jordehi, 2020)	Wind (Soroudi, 2017)	Market price at PCC ($/kWh) (Kavousi-Fard et al., 2018)
1	0.8	0	0.07867	0.230
2	0.805	0	0.08667	0.190
3	0.81	0	0.11733	0.140
4	0.818	0	0.25866	0.120
5	0.830	0.02	0.36133	0.120
6	0.910	0.1080	0.56667	0.130
7	0.950	0.2790	0.65066	0.130
8	0.970	0.5190	0.56666	0.140
9	1.000	0.7424	0.4840	0.170
10	0.980	0.9184	0.5480	0.220
11	1.000	0.9755	0.75733	0.220
12	0.970	0.9678	0.71066	0.220
13	0.950	1.0000	0.87066	0.210
14	0.900	0.9040	0.93200	0.220
15	0.905	0.8105	0.96667	0.190
16	0.910	0.6980	1.000	0.180
17	0.930	0.4675	0.86933	0.170
18	0.900	0.2520	0.66533	0.230
19	0.940	0.0940	0.65600	0.210
20	0.970	0.0200	0.56133	0.220
21	1.000	0.0010	0.56533	0.180
22	0.930	0	0.55600	0.170
23	0.900	0	0.72400	0.130
24	0.940	0	0.84000	0.120

CONOPT3 version 3.17I in GAMS has been used for solving the proposed model (Soroudi, 2017). The proposed model includes 11 blocks of equations, 15 blocks of variables, 5834 single variables and 4891 single equations. The model also includes 21225 Jacobian elements, 12288 of which are nonlinear. The computational time was 4.535 seconds and the resource limit has been set as 1000 seconds.

The simulations have been done for four different scenarios; in scenario 1, optimal power flow in the MG with VC is done considering reactive power costs. In the second scenario, optimal power flow in MG is done without

VC. In the third scenario, optimal power flow of MG is done without consideration of reactive power cost and in the fourth scenario, optimal power flow is done without controlled BSS scheduling.

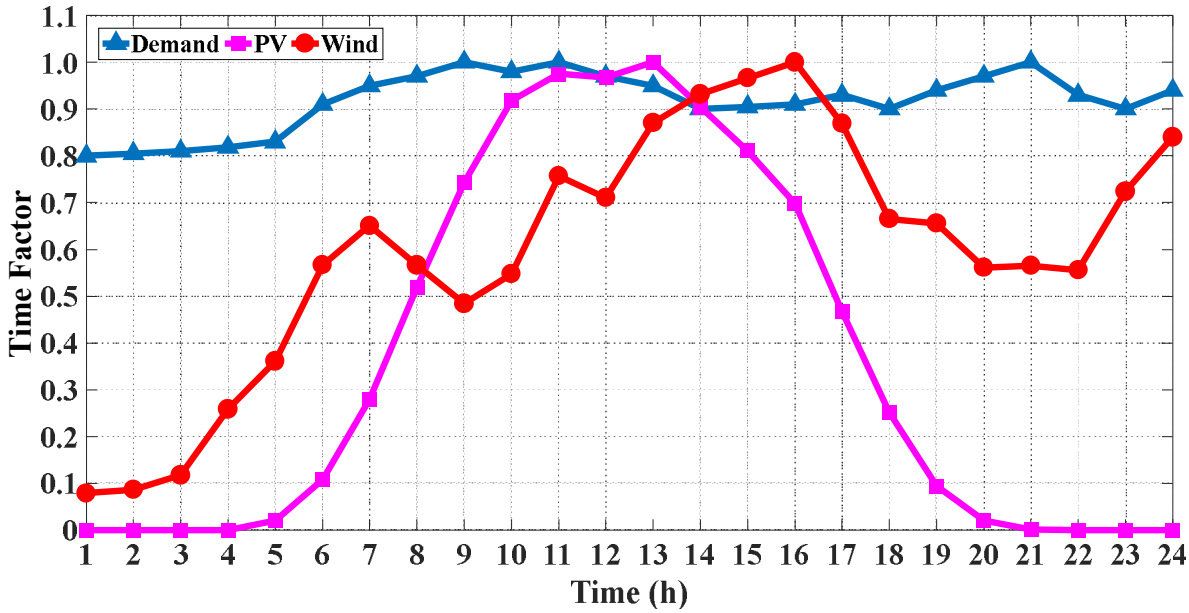

Fig.2. Time variations of demand, PV power and wind power over the hours of a day

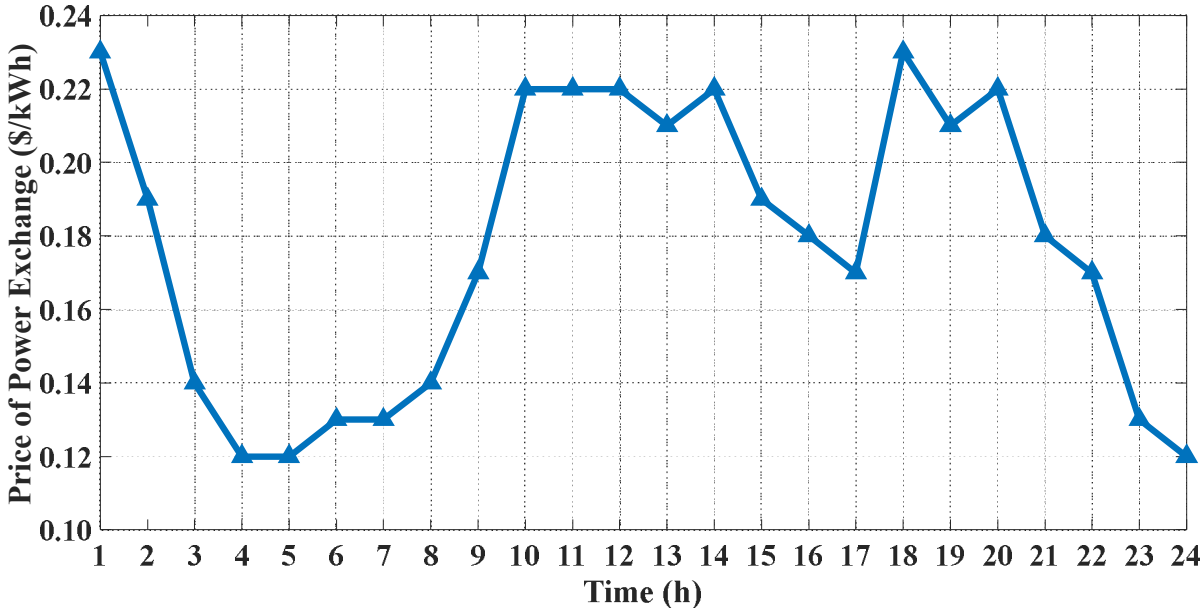

Fig.3. Time variations of market price at PCC over the horizon of a day

4.1. Optimal power flow in VC-integrated MG with BSS, considering reactive power costs

In this scenario, OPF is done in MG, while reactive power cost is considered. As per the achieved results, operation cost of the MG is $13613.9848 including $11336.941 as active power cost and $2277.0438 as reactive power cost. Load shed at all buses and all times is equal to zero. Active and reactive power dispatch of dispatchable DGs and power exchange with grid has been tabulated as Table 3.

Table 3. Active and reactive power of DGs (in pu) for different times

Hour	Grid power	Active power of DG1	Active power of DG2	Active power of DG3	Active power of DG4	Reactive power of DG1	Reactive power of DG2	Reactive power of DG3	Reactive power of DG4
1	-1.7350	2.5000	1.0000	0.3695	0.8297	1.0000	0.3887	0	0
2	-1.2599	2.5000	1.0000	0.2000	0.5297	1.0000	0.4065	0	0
3	2.0000	2.0000	0.7900	0.2000	0.2297	1.0000	0.5854	0	0
4	2.0000	1.5275	1.0000	0.2000	0.2000	1.0000	0.5714	0	0
5	2.0000	1.4796	1.0000	0.2000	0.2000	1.0000	0.6016	0	0
6	2.0000	1.5617	0.9037	0.2000	0.2000	1.0000	0.7413	0	0.0461
7	2.0000	1.5589	0.8029	0.2000	0.2000	1.0000	0.7612	0	0.1185
8	2.0000	2.0000	0.5949	0.2000	0.2000	1.0000	0.7768	0	0.1967
9	-0.21558	2.5000	0.9949	0.2000	0.2000	1.0000	0.6799	0	0.2132
10	-2.0000	2.5000	1.0000	0.2000	0.2000	1.0000	0.7018	0	0.0967
11	-2.0000	2.5000	1.0000	0.2000	0.2000	1.0000	0.7143	0	0.1416
12	-2.0000	2.5000	1.0000	0.2000	0.2000	1.0000	0.7013	0	0.0840
13	-2.0000	2.5000	1.0000	0.2000	0.2000	1.0000	0.6948	0	0.0575
14	-2.0000	2.5000	1.0000	0.2000	0.2000	1.0000	0.6418	0	0
15	-2.0000	2.5000	1.0000	0.2000	0.2000	1.0000	0.6510	0	0
16	-1.3599	2.5000	1.0000	0.2000	0.2000	1.0000	0.6684	0	0.00938
17	-0.4436	2.5000	1.0000	0.2000	0.2000	1.0000	0.6474	0	0.09925
18	-2.0000	2.5000	1.0000	0.2000	0.3617	1.0000	0.6092	0	0
19	-2.0000	2.5000	1.0000	0.2000	0.6386	1.0000	0.6760	0	0.0245
20	-2.0000	2.5000	1.0000	0.2000	0.5000	1.0000	0.6775	0	0.0940
21	-0.32793	2.5000	1.0000	0.2000	0.2000	1.0000	0.7057	0	0.1410
22	0.135543	2.5000	1.0000	0.2000	0.2000	1.0000	0.6458	0	0.0802
23	2.0000	2.0000	0.6000	0.2000	0.2000	1.0000	0.7289	0	0.0667
24	2.0000	1.6675	0.7509	0.2000	0.2000	1.0000	0.7564	0	0.1013

At hour 1 when MG demand excluding BSS is 2.9720 MW, PV units produce nothing, two wind generators generate 66.8695 MW in aggregate and grid is the most expensive source of power, it seems reasonable to fully load all dispatchable DGs and sell the extra power to the grid to make a profit. However, at this hour, upper voltage magnitude limit of bus 11 and ramp-down rate limit of DG4 are binding constraints, respectively with marginal values -17.163 $/pu and -35.99 $/MWh and do not let DG3 and DG4 to be fully loaded. Therefore, at hour 1, DG1 and DG2 are respectively loaded with 2.5 MW and 1 MW, DG3 and DG4 are partially loaded respectively with 0.3695 MW and 0.8297 MW. At this hour, MG does not miss its energy arbitrage opportunity by charging BSS, so BSS is in idle mode. If upper voltage constraints and ramp-down rate constraints are

relaxed, DG1, DG2, DG3 and DG4 would respectively generate 2.5 MW, 1 MW, 1 MW and 1 MW, more power is sold to the grid and more benefit would be achieved.

At hour 2 when MG demand excluding BSS is 2.9906 MW, market price at PCC is higher than bids of DG1 and DG2 but lower than bids of DG3 and DG4, it seems reasonable to fully load DG1 and DG2 and load DG3 and DG4 with minimum power, however, upper voltage limit of bus 11 and ramp down rate limit of DG1 and DG4 are binding constraints and make that schedule infeasible. Due to the mentioned binding constraints, the power of DG4 is 0.5297 MW rather than 0.20 MW. However, DG1 and DG2 are working with their maximum power 2.5 MW and 1 MW and DG3 is working with its minimum power and the extra 1.2599 MW is sold to the grid. In order to use energy arbitrage opportunity, BSS is not charged at this time.

During hours 3-8 when market price at PCC is cheaper than bid of all DGs, the best schedule seems to purchase the maximum power, i.e., 2 MW from grid and supply the remaining demand and BSS with dispatchable DGs according to their bids. However, for this time interval, upper voltage limit of bus 1 is a binding constraint and does not allow the mentioned schedule. At hour 3 when MG demand without BSS is 3.0092 MW, DG1, DG2, DG3 and DG4 are operating respectively with 2 MW, 0.79 MW, 0.20 MW and 0.2297 MW and BSS is in charging mode with its maximum charging power, i.e., 2 MW. At hour 3, ramp-down rate limit of DG4 does not let its power to fall below 0.2297 MW. Thanks to the cheap price of grid power at hours 3-8, this time interval is suitable to charge BSS, so as Table 3 shows, at these hours, BSS operates in charging mode.

At hour 9 when market price at PCC is higher than bid of DG1 and DG2 but lower than bid of DG4 and DG3, it seems reasonable to fully load DG1 and DG2 and load DG3 and DG4 with minimum power and sell back the extra power to the grid, however ramp-up rate limit of DG2 does not allow its power to be higher than 0.9949 MW. Therefore, DG1, DG2, DG3 and DG4 respectively produce 2.5 MW, 0.9949 MW, 0.2 MW and 0.2 MW, PV and wind units produce 668.160 kW and 411.40 kW. With the mentioned generation of dispatchable and renewable DGs, 3.7150 MW demand of MG is fed, the maximum possible power, i.e., 2 MW is sold to the grid and the extra 0.894 MW is used to charge BSS.

At hours 10-12, market price at PCC is higher than bid of all DGs, but by fully loading the cheapest DGs, i.e., DG1 and DG2, MG is able to sell the maximum possible power to the grid and loading DG3 and DG4 with more than their minimum power does not increase energy arbitrage opportunity and benefit of MG. On the other hand, it is not economical to charge BSS with expensive DGs, i.e., DG3 and DG4. Therefore, at these hours, DG1 and DG2 operate with their maximum power, DG3 and DG4 operate with minimum power and BSS is discharged respectively with 0.536 MW, 0.396 MW and 0.328 MW at hour 10, 11 and 12.

At hours 13-14, due to high generation of renewable DGs, loading DG3 and DG4 with higher than minimum power is not economical. At hour 13, even charging BSS with DG3 and DG4 is not economical and BSS is operating in its discharging mode. At hour 13, PV units generate their peak power and produce 900 kW in aggregate and wind units are generating 740.0610 kW. Therefore, at hours 13-14, DG1 and DG2 are fully loaded and DG3 and DG4 are loaded with minimum power.

At hours 15-17 when market price at PCC is higher than bids of DG1 and DG2 and lower than bids of DG3 and DG4, it is rational to fully load DG1 and DG2 and load DG3 and DG4 with minimum power. At hour 15, the maximum possible power is exported to the grid and at hours 16 and 17 MG is respectively exporting 1.3599 MW and 0.4436 MW to the grid. At hours 18-20, market price at PCC is higher than bids of DG1, DG2 and DG3, so it is the right time to fully load cheap DGs, i.e., DG1 and DG2 and export the maximum possible power to the grid. At these hours, BSS is in its discharging mode to enhance energy arbitrage capability of the MG. At hours 21-22, market price at PCC is higher than bids of DG1 and DG2, but lower than bids of DG3 and DG4, so DG1 and DG2 must be fully loaded and DG3 and DG4 must be loaded with their minimum power.

At hour 23, market price decreases and gets lower than bid of all DGs, so the maximum possible power is purchased from grid and DG1 and DG2 that were fully loaded at previous time, must be loaded with minimum power. However, due to ramp-down rate limit of DG1 and DG2, their power cannot respectively fall below 2 MW and 0.6 MW. At hour 24, again grid power is the cheapest source of power for MG and the maximum

possible power is imported from grid to supply demand and charge BSS. At hours 23 and 24, upper voltage limit of bus 1 is a binding constraint.

Regarding reactive power dispatch in MG, DG1 is the cheapest resource of reactive power, followed by DG2, VC, DG4 and DG3. However, in hours 1-2, VC is supplying a portion of reactive power demand, while the reactive power of DG2 is not fully utilised, or in later hours, the maximum reactive power of VC is used, while reactive power of DG2 is partially used. The reason is that upper voltage limit constraint in some buses is binding and does not allow the most economical dispatch. At hours 1-2, upper voltage limit of bus 11, at hours 3-8, upper voltage limit of bus 1, at hours 9-17, upper voltage limit of bus 18, at hours 18, upper voltage limit of bus 17 and at hours 19-22, upper voltage limit of bus 12 are binding constraints. Voltages of some selected buses at different hours have been tabulated as Table 4.

To have an idea how shadow price changes with time, the shadow price of active and reactive power at different hours have been tabulated as Table 5. Actually this table includes shadow prices at bus 1. The difference between shadow prices of active/reactive power in different buses of a power system may be caused either by either active/reactive power congestion or active/reactive power loss in branches. For this MG, as there is no congestion in branches, there is only a negligible difference between local marginal prices of active/reactive power at different buses. The changes in locational marginal price (LMP) over time is mainly due to changes in market price at PCC and the changes in equivalent active power demand of the MG, which is defined as active power demand of MG minus power generated by renewable power resources. On the other hand, the change in local marginal reactive power price (LMQ) over time is mainly due to changes in reactive power demand of the MG.

Table 4. Voltages of buses with dispatchable DGs (in pu) for different times

Hour	Voltage bus #1	Voltage bus #2	Voltage bus #11	Voltage bus #15	Voltage bus #27	Hour	Voltage bus #1	Voltage bus #2	Voltage bus #11	Voltage bus #15	Voltage bus #27
1	1.0782	1.0791	1.1000	1.0988	1.0793	13	1.0399	1.0410	1.0871	1.0937	1.0410
2	1.0876	1.0883	1.1000	1.0960	1.0820	14	1.0399	1.0410	1.0869	1.0939	1.0400
3	1.1000	1.0990	1.0782	1.0742	1.0536	15	1.0403	1.0414	1.0878	1.0944	1.0412

4	1.1000	1.0990	1.0909	1.0880	1.0597	16	1.0493	1.0500	1.0890	1.0949	1.0409
5	1.1000	1.0990	1.0941	1.0919	1.0603	17	1.0696	1.0698	1.0937	1.0970	1.0498
6	1.1000	1.0990	1.0977	1.0967	1.0606	18	1.0603	1.0614	1.0982	1.0990	1.0657
7	1.1000	1.0990	1.0980	1.0984	1.0607	19	1.0614	1.0625	1.0995	1.0988	1.0691
8	1.1000	1.0990	1.0879	1.0891	1.0541	20	1.0640	1.0651	1.0998	1.0976	1.0734
9	1.0800	1.0801	1.0953	1.0971	1.0581	21	1.0845	1.0847	1.0999	1.0973	1.0694
10	1.0517	1.0528	1.0920	1.0956	1.0550	22	1.0911	1.0910	1.0998	1.0978	1.0670
11	1.0443	1.0454	1.0893	1.0945	1.0474	23	1.1000	1.0990	1.0881	1.0876	1.0553
12	1.0456	1.0467	1.0895	1.0946	1.0479	24	1.1000	1.0990	1.0979	1.0978	1.0605

Table 5. Shadow price of active power and reactive power at bus #1 (in $/pu) for different times

Hour	Active power price at bus #1	Reactive power price at bus #1	Hour	Active power price at bus #1	Reactive power price at bus #1
1	0.2300	0.0427	13	0.1905	0.0457
2	0.1900	0.0431	14	0.1888	0.0452
3	0.1478	0.0441	15	0.1899	0.0453
4	0.1536	0.0439	16	0.1800	0.0456
5	0.1536	0.0441	17	0.1700	0.0459
6	0.1536	0.0452	18	0.1978	0.0450
7	0.1536	0.0454	19	0.1988	0.0457
8	0.1428	0.0454	20	0.2034	0.0458
9	0.1700	0.0462	21	0.1800	0.0461
10	0.1960	0.0458	22	0.1700	0.0460
11	0.1942	0.0459	23	0.1495	0.0452
12	0.1933	0.0458	24	0.1536	0.0454

Table 6 contains power exchange between MG and BSS as well as energy level of BSS at different times. As per this table, hours such as 3-9 or 22-24, when market price at PCC is low, are appropriate times for charging BSS, because at these times MG is able to purchase maximum transferable power from grid and can charge BSS with low cost. For instance, at hour 3 when market price at PCC is as low as 140 $/MWh, BSS is charged with maximum charging power, i.e., 2 MW and its energy level reaches 2000 kWh.

Table 6. Power exchange between MG and BSS, operation mode and energy level of BSS at different times

Hour	BSS operation mode	BSS power (pu)	BSS Energy (kWh)
1	Idle	0	0
2	Idle	0	0
3	Charging	2	2000
4	Charging	1.841	3841.105
5	Charging	1.851	5691.941

6	Charging	1.787	7479.184
7	Charging	1.759	9237.824
8	Charging	2	11237.824
9	Charging	0.894	12131.571
10	Discharging	-0.536	11595.589
11	Discharging	-0.396	11199.453
12	Discharging	-0.328	10871.093
13	Discharging	-0.105	10766.397
14	Charging	0.043	10809.083
15	Discharging	-0.028	10780.986
16	Charging	0.502	11283.259
17	Charging	0.997	12279.786
18	Discharging	-0.569	11710.989
19	Discharging	-0.591	11119.629
20	Discharging	-0.990	10129.136
21	Charging	0.245	10373.902
22	Charging	0.911	11285.029
23	Charging	1.955	13239.620
24	Charging	1.760	15000

On the other hand, in hours such as 10-13 or 18-20 when market price is high, BSS is in its discharging mode to enhance export capability of MG and reduce MG operation cost. According to Table 6, at the end of operation horizon, energy level of BSS reaches the target 15000 kWh.

Table 7 shows hourly reactive power that MG purchases from VC. After DG1 and DG2, VC is the cheapest resource of reactive power for MG. However, in hours 1-2, VC is supplying a portion of reactive power demand, while the reactive power of DG2 is not fully used, or in later hours, MG purchases maximum reactive power of VC, while reactive power of DG2 is partially used. The reason is that upper voltage limit constraint in some buses is binding and precludes the most economical dispatch. Actually, VC not only decreases MG operation cost, but also enhances voltage stability of the MG.

Fig.4 and Fig.5 respectively illustrate active and reactive power dispatch of MG resources. Fig.6. shows voltage variations of buses with dispatchable DGs. Fig.7 and Fig.8 respectively show shadow price of active and reactive power at bus 1. Fig.9 and Fig.10 respectively illustrate hourly changes of BSS power and energy and Fig.11 shows the share of VC in provision of MG reactive power at different hours.

Table 7. Reactive power purchased from VC at different times

Hour	Reactive power (in pu)	Hour	Reactive power (in pu)
1	0.477	13	0.5
2	0.466	14	0.5
3	0.5	15	0.5
4	0.5	16	0.5
5	0.5	17	0.5
6	0.5	18	0.5
7	0.5	19	0.5
8	0.5	20	0.5
9	0.5	21	0.5
10	0.5	22	0.5
11	0.5	23	0.5
12	0.5	24	0.5

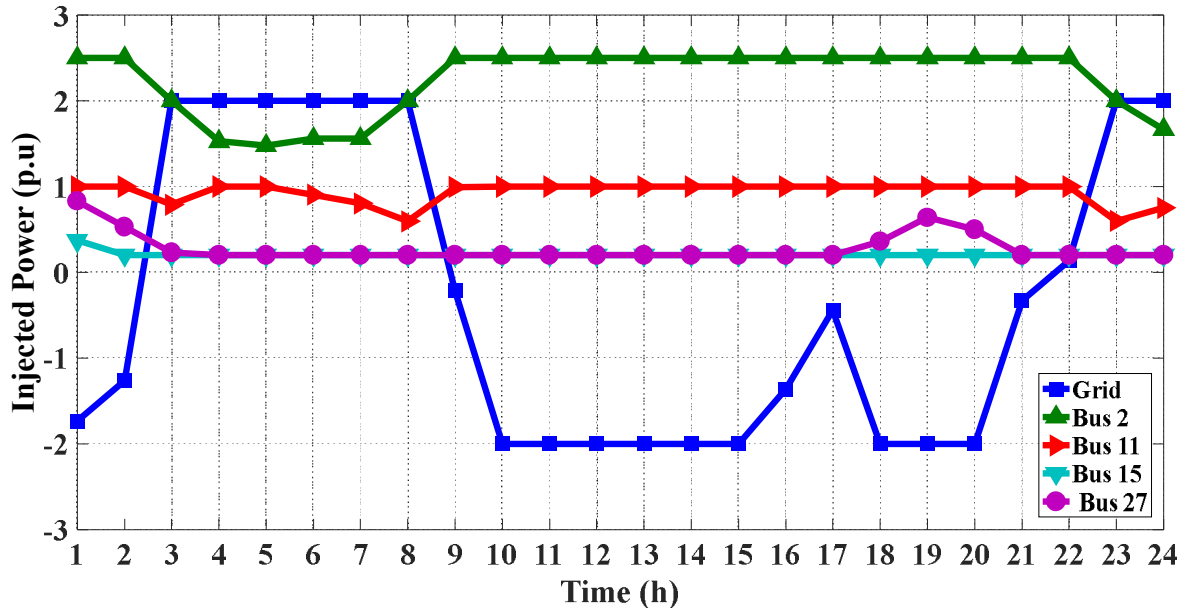

Fig.4. Optimal dispatch of dispatchable DGs and power exchange with grid

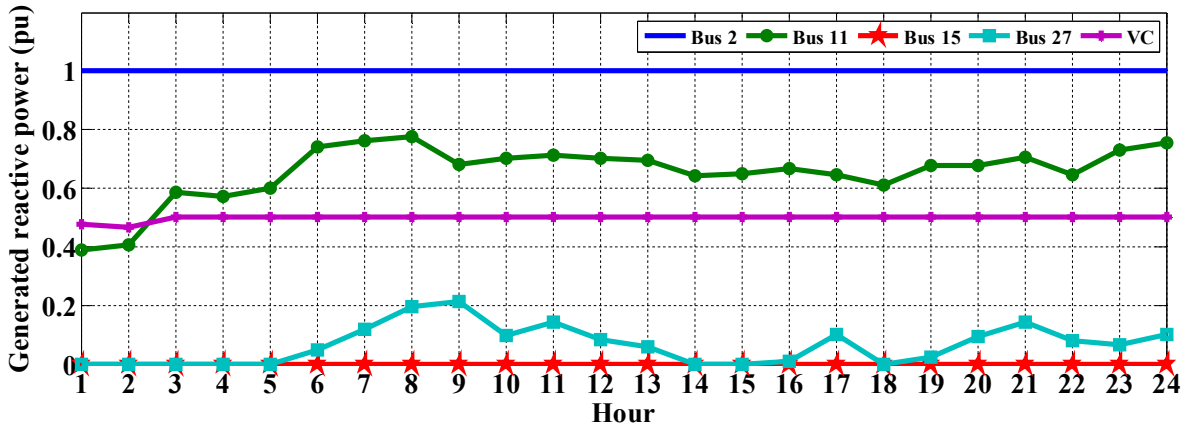

Fig.5. Optimal reactive power dispatch of dispatchable DGs and VC

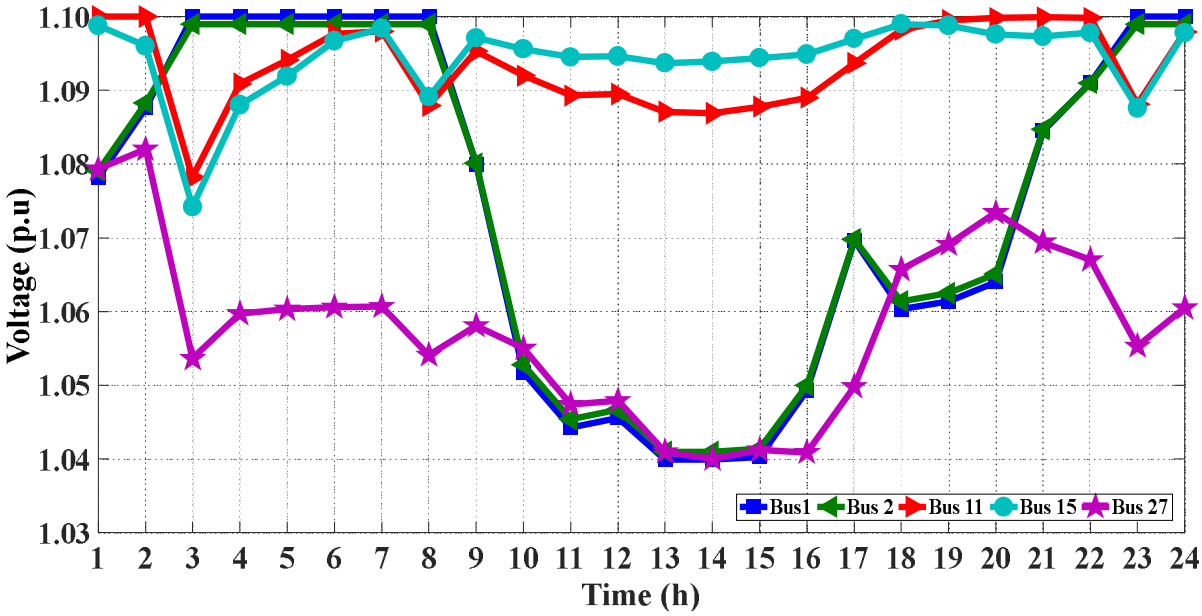

Fig.6. Voltage variations of buses with dispatchable DGs in scenario 1

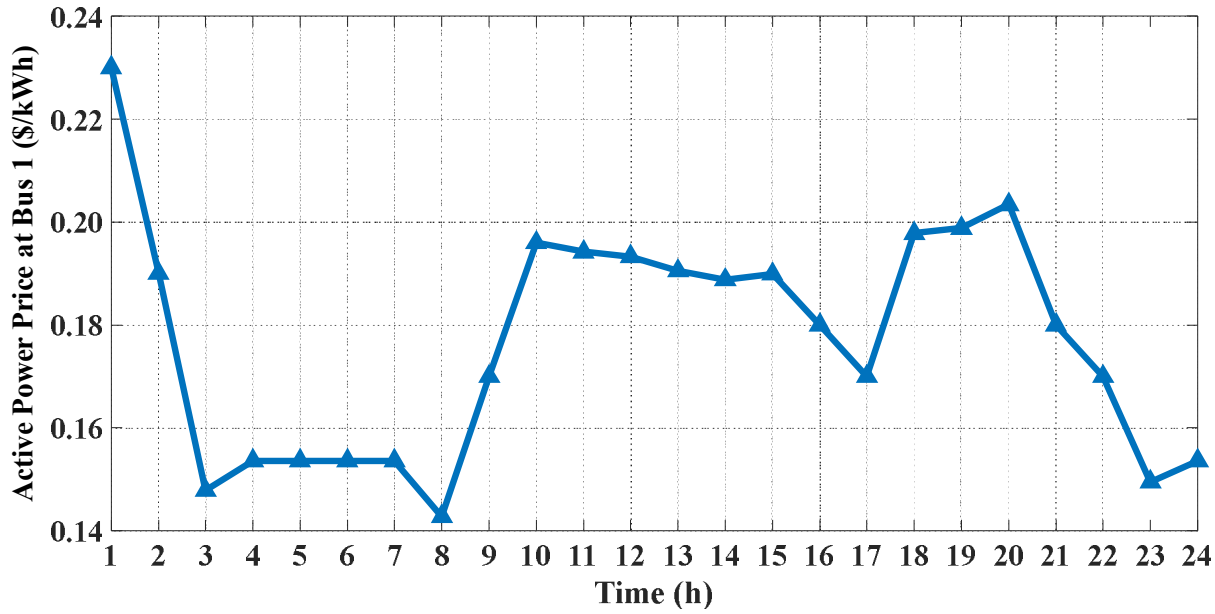

Fig.7. Shadow price of active power at bus #1 for scenario 1

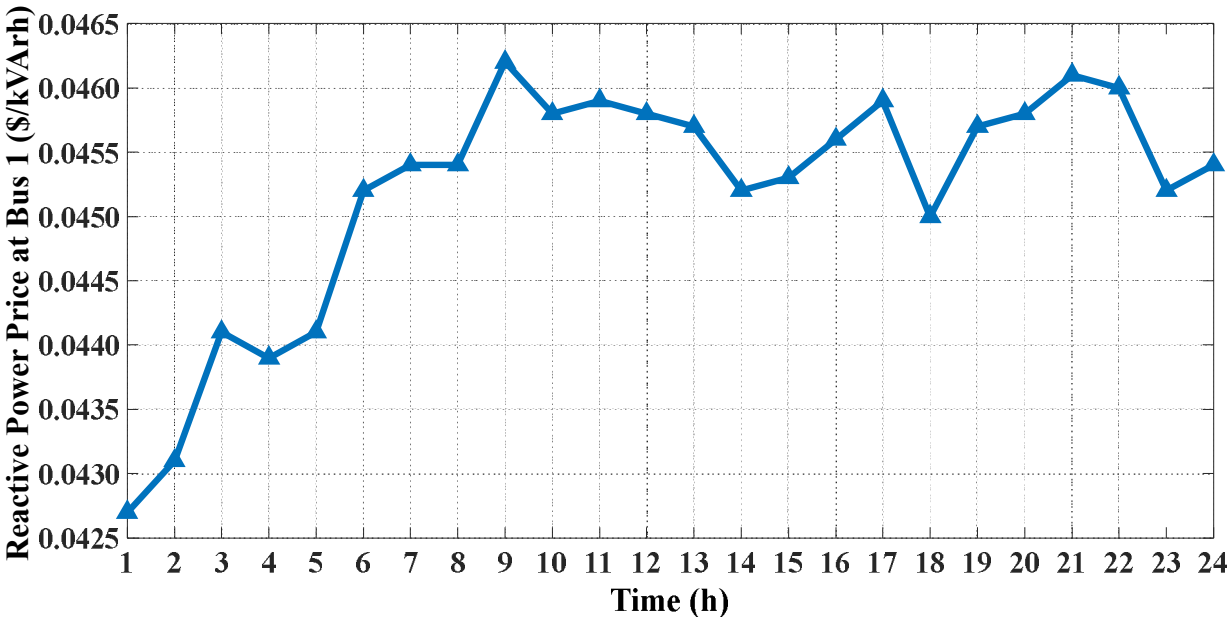

Fig.8. Shadow price of reactive power at bus #1 for scenario 1

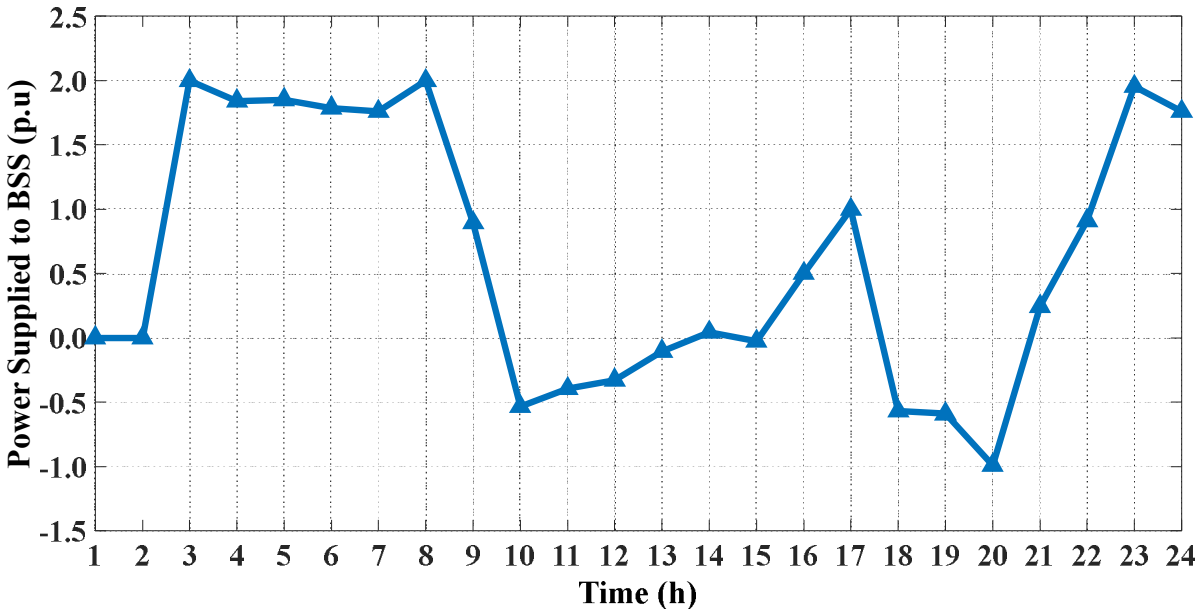

Fig.9. BSS absorbed power at different hours for scenario 1

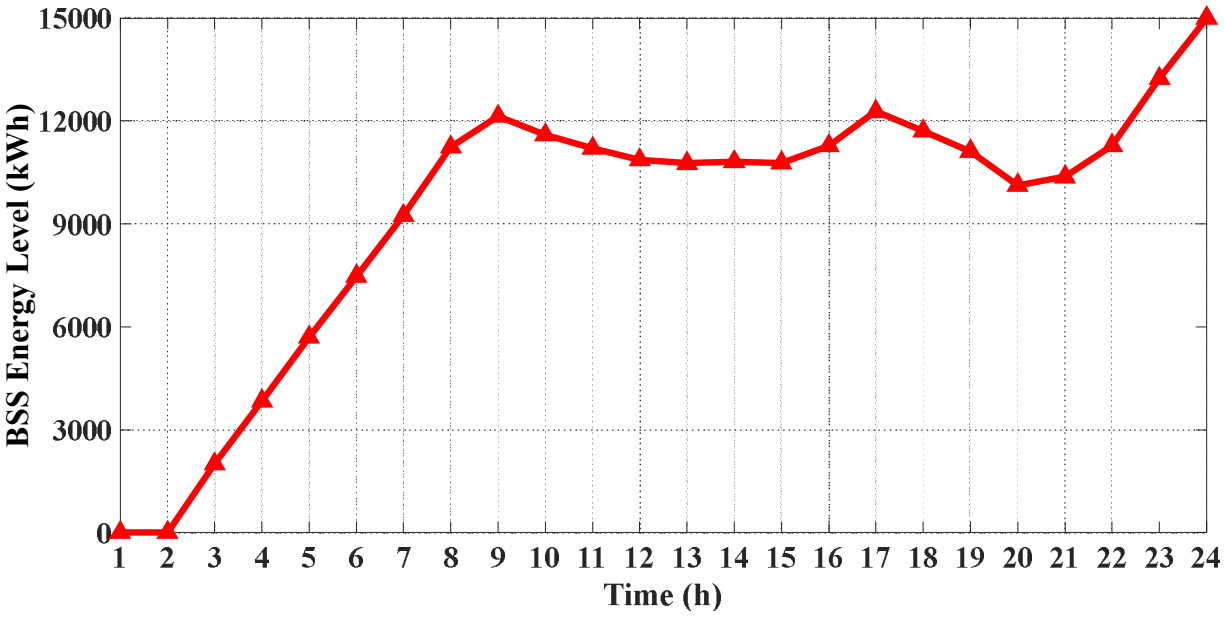

Fig.10. BSS energy level at different hours for scenario 1

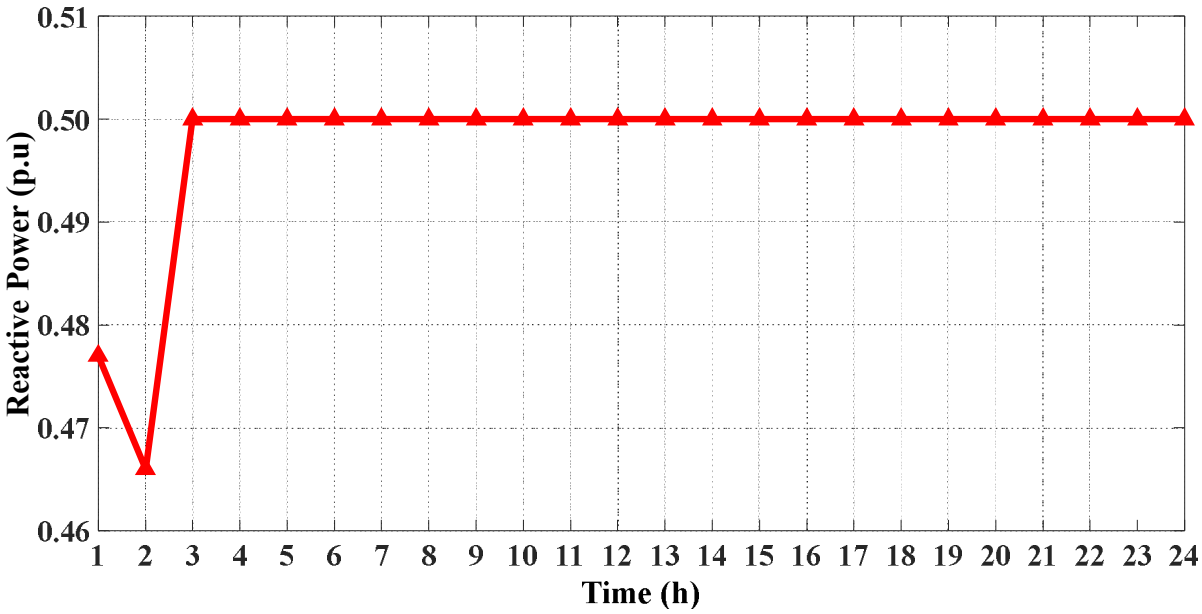

Fig.11. Reactive power purchased from VC at different hours

4.2. Optimal power flow in BSS-integrated MG without VC

In this scenario, in order to investigate the effect of VC on MG operation cost, shadow prices and reactive power dispatch, optimal power flow has been done without VC. In scenario 1, with VC, MG operation cost was $13613.985 including $11336.941 as active power cost and $2277.0438 as reactive power cost. The simulation results show that in this scenario, MG operation cost is $13695.1592, including $11404.263 for real power and $2290.8962 for reactive power. The results indicate that VC decreases both reactive power cost and active power cost of MG. VC reduces MG reactive power cost, because at most of the times, reactive power resources such as DG3 and DG4 are replaced with VC as a cheaper reactive power source. On the other hand, through reduction of power loss, VC decreases active power cost of MG. Table 8 compares shadow prices of reactive power with and without VC. The table shows that at all time periods, shadow price of reactive power in MG with VC is less than shadow price without VC. The average of shadow prices of reactive power with and without VC are respectively 0.0452 $/kWh and 0.0506 $/kWh which shows that VC has reduced shadow price of reactive power by 10.67%. Reactive power dispatch in this scenario can be found in Table 9.

Table 8. Comparison of Shadow price of reactive power at bus #1 (in $/pu) for different times

Hour	With VC	Without VC	Hour	With VC	Without VC
1	0.0427	0.0448	13	0.0457	0.0485
2	0.0431	0.0452	14	0.0452	0.0473
3	0.0441	0.0458	15	0.0453	0.0475
4	0.0439	0.0457	16	0.0456	0.0479
5	0.0441	0.0459	17	0.0459	0.0490
6	0.0452	0.0488	18	0.0450	0.0471
7	0.0454	0.0581	19	0.0457	0.0481
8	0.0454	0.0622	20	0.0458	0.0491
9	0.0462	0.0579	21	0.0461	0.0561
10	0.0458	0.0555	22	0.0460	0.0489
11	0.0459	0.0566	23	0.0452	0.0536
12	0.0458	0.0489	24	0.0454	0.0570

Table 9. Reactive power of DGs (in pu) in MG without VC

Hour	DG1	DG2	DG3	DG4	Hour	DG1	DG2	DG3	DG4
1	1	0.5714	0	0.3	13	1	0.9631	0	0.3
2	1	0.6177	0	0.260926	14	1	0.8505	0	0.3
3	1	0.7964	0	0.3	15	1	0.8607	0	0.3
4	1	0.7821	0	0.3	16	1	0.8894	0	0.3
5	1	0.8126	0	0.3	17	1	0.9603	0	0.3
6	1	1.0000	0	0.3	18	1	0.8174	0	0.3
7	1	1.0000	0.0842	0.3	19	1	0.9101	0	0.3
8	1	1.0000	0.1891	0.3	20	1	0.9835	0	0.3
9	1	1.0000	0.1059	0.3	21	1	1.0000	0	0.3
10	1	1.0000	0.0106	0.3	22	1	0.9393	0	0.3
11	1	1.0000	0.0694	0.3	23	1	1	0.00793	0.3
12	1	0.9970	0	0.3	24	1	1	0.062345	0.3

The table shows that the dispatch of reactive power is not only affected by economical reasons but also by voltage and ramp constraints. For instance, at hour 1, although reactive power bid of DG4 is higher than that of DG2, DG4 supplies 0.3 MVar, while DG2 has not supplied its maximum reactive power. The voltages of buses with DGs in the MG without VC can be found in Table 10.

Table 10. Voltages of buses with dispatchable DGs

Hour	Voltage bus #1	Voltage bus #2	Voltage bus #11	Voltage bus #15	Voltage bus #27	Hour	Voltage bus #1	Voltage bus #2	Voltage bus #11	Voltage bus #15	Voltage bus #27
1	1.0749	1.0758	1.1000	1.0987	1.0757	13	1.0345	1.0356	1.0871	1.0937	1.0353
2	1.0835	1.0841	1.1000	1.0960	1.0776	14	1.0357	1.0368	1.0869	1.0939	1.0355
3	1.1000	1.0990	1.0823	1.0784	1.0533	15	1.0369	1.0379	1.0878	1.0944	1.0365
4	1.1000	1.0990	1.0948	1.0919	1.0592	16	1.0454	1.0462	1.0890	1.0949	1.0360
5	1.1000	1.0990	1.0980	1.0958	1.0598	17	1.0637	1.0639	1.0937	1.0970	1.0431
6	1.1000	1.0990	1.0997	1.0987	1.0592	18	1.0562	1.0573	1.0982	1.0990	1.0613
7	1.1000	1.0990	1.0975	1.0991	1.0589	19	1.0568	1.0579	1.0995	1.0988	1.0643
8	1.0986	1.0976	1.0941	1.0980	1.0521	20	1.0580	1.0591	1.0998	1.0976	1.0671
9	1.0702	1.0703	1.0937	1.0971	1.0478	21	1.0780	1.0782	1.0998	1.0981	1.0618
10	1.0454	1.0465	1.0919	1.0956	1.0484	22	1.0858	1.0857	1.0998	1.0978	1.0608
11	1.0362	1.0373	1.0883	1.0945	1.0388	23	1.1000	1.0990	1.0934	1.0930	1.0549
12	1.0397	1.0409	1.0895	1.0946	1.0417	24	1.1000	1.0990	1.0988	1.0996	1.0592

4.3. Optimal power flow in VC-integrated MG with BSS without consideration of reactive power costs

In this scenario, optimal power flow in MG is done without considering reactive power costs. In such a scenario, reactive power resources are dispatched in a way that the power loss of the MG and thereby its operation cost is minimised. Reactive power dispatch of DGs has been tabulated as Table 11.

Table 11. Reactive power dispatch of DGs (in pu) without consideration of reactive power cost

Hour	DG1	DG2	DG3	DG4	Hour	DG1	DG2	DG3	DG4
1	0.7061	0.2479	0.1128	0.3	13	0.9478	0.4000	0.1023	0.3
2	0.7095	0.2158	0.1456	0.3	14	0.8768	0.3752	0.0875	0.3
3	0.7994	0.3372	0.1465	0.3	15	0.8827	0.3759	0.0901	0.3
4	0.7992	0.3493	0.1477	0.3	16	0.9073	0.3862	0.0768	0.3
5	0.8146	0.3601	0.1498	0.3	17	1.0000	0.4100	0.0360	0.3
6	0.9366	0.4172	0.1644	0.3	18	0.8630	0.3282	0.1170	0.3
7	0.9966	0.4414	0.1723	0.3	19	0.9317	0.3517	0.1204	0.3
8	1.0000	0.4948	0.1769	0.3	20	0.9810	0.3189	0.1726	0.3
9	1.0000	0.5249	0.0669	0.3	21	1.0000	0.3612	0.1780	0.3
10	0.9805	0.3852	0.1308	0.3	22	0.9956	0.2690	0.1601	0.3
11	1.0000	0.4317	0.1225	0.3	23	0.9327	0.4047	0.1627	0.3
12	0.9700	0.3940	0.1192	0.3	24	0.9827	0.4355	0.1701	0.3

In this scenario, reactive power limit of DG4 is a binding constraint and operation cost of MG is $11319.543. Comparing the results with scenario 1 shows that ignoring reactive power cost in dispatch of MG resources decreases MG operation cost from $11336.941 to $11319.543. The reason is that with ignoring reactive power costs, reactive power resources are dispatched in a way that power loss of MG and thereby its active power cost is reduced.

4.4. Optimal power flow in VC-integrated MG with BSS, without controlled scheduling of BSS

In this scenario, in order to see the effect of optimal scheduling of BSS in MG, it is assumed that BSS is charging its batteries with a constant power. To fully charge all its batteries, BSS must absorb a constant 312.5 kW power at all hours. The MG operation cost in this scenario is $14025.4394, while with optimal BSS scheduling it was $13613.9848. This indicates that optimal BSS scheduling decreases $412, namely 2.93% of MG operation cost.

Table 12 compares shadow prices with and without optimal BSS scheduling in MG. According to this table, at hours with lower market prices, such as 3-4 or 23-24, optimal BSS scheduling increases shadow prices. This is due to the fact that at these hours, with optimal BSS scheduling, BSS absorbs a high charging power from MG that significantly increases MG demand and increases shadow price.

On the other hand, at hours with higher market prices, such as 18-20, optimal BSS scheduling decreases shadow prices, because at these hours, with optimal BSS scheduling, BSS injects its discharging power to the MG that significantly decreases MG demand and thereby decreases shadow price. The average shadow price with and without optimal BSS scheduling are respectively 177.1 $/MWh and 179.1 $/MWh which shows that optimal BSS scheduling decreases shadow prices by 11.1%.

Table 12. Comparison of shadow price of active power at bus #1 (in $/pu) with and without optimal BSS scheduling

Hour	With optimal BSS scheduling	Without optimal BSS scheduling	Hour	With optimal BSS scheduling	Without optimal BSS scheduling
1	0.2300	0.2300	13	0.1905	0.1959
2	0.1900	0.1900	14	0.1888	0.1990
3	0.1478	0.1400	15	0.1899	0.1900
4	0.1536	0.1200	16	0.1800	0.1800
5	0.1536	0.1537	17	0.1700	0.1700
6	0.1536	0.1536	18	0.1978	0.2300
7	0.1536	0.1300	19	0.1988	0.2100
8	0.1428	0.1400	20	0.2034	0.2200
9	0.1700	0.1700	21	0.1800	0.1800
10	0.1960	0.2200	22	0.1700	0.1700
11	0.1942	0.2200	23	0.1495	0.1300
12	0.1933	0.2200	24	0.1536	0.1354

Table 13 and 14 respectively show voltages and power dispatch in this scenario. Comparison of table 14 and table 3 indicates that optimal BSS scheduling significantly affects dispatch of power resources in MG. load shed at all buses and times is zero.

Table 13. Voltages of buses with dispatchable DGs (in pu) without optimal BSS scheduling

Hour	Voltage bus #1	Voltage bus #2	Voltage bus #11	Voltage bus #15	Voltage bus #27	Hour	Voltage bus #1	Voltage bus #2	Voltage bus #11	Voltage bus #15	Voltage bus #27
1	1.0814	1.0820	1.0991	1.1000	1.0736	13	1.0406	1.0417	1.0871	1.0937	1.0417
2	1.0964	1.0964	1.1000	1.0960	1.0803	14	1.0400	1.0411	1.0869	1.0939	1.0402
3	1.1000	1.0994	1.0871	1.0832	1.0743	15	1.0452	1.0461	1.0878	1.0944	1.0402
4	1.1000	1.0990	1.0804	1.0774	1.0715	16	1.0485	1.0492	1.0890	1.0949	1.0412
5	1.1000	1.0990	1.0902	1.0880	1.0748	17	1.0573	1.0580	1.0937	1.0970	1.0515
6	1.1000	1.0990	1.0940	1.0930	1.0740	18	1.0680	1.0688	1.0982	1.0990	1.0644
7	1.1000	1.0991	1.0953	1.0956	1.0736	19	1.0734	1.0740	1.0995	1.0988	1.0676
8	1.1000	1.0994	1.0966	1.0978	1.0739	20	1.0792	1.0797	1.0998	1.0976	1.0712
9	1.0827	1.0827	1.0953	1.0971	1.0661	21	1.0836	1.0837	1.0999	1.0973	1.0699
10	1.0606	1.0613	1.0920	1.0956	1.0547	22	1.0952	1.0949	1.0998	1.0978	1.0749
11	1.0489	1.0499	1.0893	1.0945	1.0481	23	1.1000	1.0992	1.0936	1.0930	1.0742
12	1.0493	1.0503	1.0895	1.0946	1.0488	24	1.1000	1.0990	1.0966	1.0965	1.0739

Table 14. Active power of DGs (in pu) without optimal BSS scheduling

Hour	Grid power	DG1	DG2	DG3	DG4	Hour	Grid power	DG1	DG2	DG3	DG4
1	-1.1767	2.5000	1.0000	0.4925	0.8000	13	-2.0000	2.5000	1.0000	0.2000	0.9579
2	-0.0752	2.0000	1.0000	0.2000	0.5000	14	-2.0000	2.5000	1.0000	0.2000	0.8065
3	1.1311	1.5000	0.6000	0.2000	0.2000	15	-1.6283	2.5000	1.0000	0.2000	0.5065
4	1.8483	1.0000	0.3000	0.2000	0.2000	16	-1.4313	2.5000	1.0000	0.2000	0.4000
5	2.0000	0.5771	0.5044	0.2000	0.2000	17	-1.3555	2.5000	1.0000	0.2000	0.7000
6	2.0000	0.7301	0.4069	0.2000	0.2000	18	-1.4195	2.5000	1.0000	0.2000	1.0000
7	1.7660	1.0000	0.3000	0.2000	0.2000	19	-1.1216	2.5000	1.0000	0.2000	1.0000
8	1.1966	1.5000	0.3000	0.2000	0.2000	20	-0.8654	2.5000	1.0000	0.2000	1.0000
9	-0.0314	2.0000	0.7000	0.2000	0.5000	21	-0.2520	2.3197	1.0000	0.2000	0.7000
10	-1.4087	2.5000	1.0000	0.2000	0.8000	22	0.5916	1.8197	0.7000	0.2000	0.4000
11	-1.7480	2.5000	1.0000	0.2000	1.0000	23	1.4424	1.3197	0.3000	0.2000	0.2000
12	-1.8168	2.5000	1.0000	0.2000	1.0000	24	2.0000	0.8197	0.3000	0.2000	0.2000

5. Conclusions

In this paper, optimal power flow has been considered in a MG including BSS, dispatchable DGs, PV and wind units, and also VC. AC power flow has been implemented to take into account reactive power dispatch and power loss, while the reactive power cost of MG has been considered in the objective function. The results showed that at hours with a low price at PCC, the BSS absorbs power from the MG and charges its stock batteries, while at hours with a high price at PCC, the BSS discharges its batteries to inject power to the MG, enhancing energy arbitrage capability and the profit of the MG. The results showed that the VC significantly reduced operation cost of the MG, either by reducing the power loss of the MG or by serving as a reactive power resource cheaper than the DGs. The results indicated that the consideration of reactive power costs in the objective function increased the active power cost of the MG. The results also showed that the optimal scheduling of the BSS significantly decreased the MG operation cost.

Acknowledgement

J.P.S. Catalão acknowledges the support by FEDER funds through COMPETE 2020 and by Portuguese funds through FCT, under POCI-01-0145-FEDER-029803 (02/SAICT/2017).

References

Auto & Mobility Trends in 2019, Available at https://www.cbinsights.com/research/report/auto-mobility-trends-2019/.
https://batteryuniversity.com/learn/article/electric_vehicle_ev.
National eclectic mobility mission plan, http://dhi.nic.in/UserView/index?mid¼1347.
Tesla 90-Second Battery Swap Tech Coming This Year, Available at Tesla 90-Second Battery Swap Tech Coming This Year.
Amiri, S.S., Jadid, S., Saboori, H., 2018. Multi-objective optimum charging management of electric vehicles through battery swapping stations. Energy 165, 549-562.
Drud, A., 1985. CONOPT: A GRG code for large sparse dynamic nonlinear optimization problems. Mathematical Programming 31, 153-191.
Drud, A.S., 1994. CONOPT—a large-scale GRG code. ORSA Journal on computing 6, 207-216.
Gao, Y.-j., Zhao, K.-x., Wang, C., 2012. Economic dispatch containing wind power and electric vehicle battery swap station, PES T&D 2012. IEEE, pp. 1-7.
Han, S., Han, S., Sezaki, K., 2010. Development of an optimal vehicle-to-grid aggregator for frequency regulation. IEEE Transactions on smart grid 1, 65-72.
Islam, M.M., Zhong, X., Sun, Z., Xiong, H., Hu, W., 2019. Real-time frequency regulation using aggregated electric vehicles in smart grid. Computers & Industrial Engineering 134, 11-26.
Javadi, M.S., Nezhad, A.E., Siano, P., Shafie-khah, M., Catalão, J.P., 2017. Shunt capacitor placement in radial distribution networks considering switching transients decision making approach. International Journal of Electrical Power & Energy Systems 92, 167-180.
Jordehi, A.R., 2020a. Dynamic environmental-economic load dispatch in grid-connected microgrids with demand response programs considering the uncertainties of demand, renewable generation and market price. International Journal of Numerical Modelling: Electronic Networks, Devices and Fields.
Jordehi, A.R., 2020b. Mixed binary-continuous particle swarm optimisation algorithm for unit commitment in microgrids considering uncertainties and emissions. International Transactions on Electrical Energy Systems.
Kavousi-Fard, A., Zare, A., Khodaei, A., 2018. Effective dynamic scheduling of reconfigurable microgrids. IEEE Transactions on Power Systems 33, 5519-5530.
Khodaei, A., 2013. Microgrid optimal scheduling with multi-period islanding constraints. IEEE Transactions on Power Systems 29, 1383-1392.
Li, Y., Yang, Z., Li, G., Mu, Y., Zhao, D., Chen, C., Shen, B., 2018. Optimal scheduling of isolated microgrid with an electric vehicle battery swapping station in multi-stakeholder scenarios: A bi-level programming approach via real-time pricing. Applied energy 232, 54-68.
Liang, Y., Zhang, X., 2018. Battery swap pricing and charging strategy for electric taxis in China. Energy 147, 561-577.
Mahoor, M., Hosseini, Z.S., Khodaei, A., 2019. Least-cost operation of a battery swapping station with random customer requests. Energy 172, 913-921.
Meral, M.E., Çelík, D., 2019. A comprehensive survey on control strategies of distributed generation power systems under normal and abnormal conditions. Annual Reviews in Control 47, 112-132.
Moaidi, F., Golkar, M.A., 2019. Demand Response Application of Battery Swap Station Using A Stochastic Model, 2019 IEEE Milan PowerTech. IEEE, pp. 1-6.
Rezaee Jordehi, A., 2020. Particle swarm optimisation with opposition learning-based strategy: An efficient optimisation algorithm for day-ahead scheduling and reconfiguration in active distribution systems. Soft computing.
Shirmohammadi, D., Hong, H.W., 1989. Reconfiguration of electric distribution networks for resistive line losses reduction. IEEE Transactions on Power Delivery 4, 1492-1498.
Soroudi, A., 2017. Power system optimization modeling in GAMS. Springer.
Turksoy, O., Yilmaz, U., Teke, A., 2019. Minimizing Capacitance Value of Interleaved Power Factor Corrected Boost Converter for Battery Charger in Electric Vehicles. Elektronika ir Elektrotechnika 25, 11-17.
Wang, Y., Lai, K., Chen, F., Li, Z., Hu, C., 2019. Shadow price based co-ordination methods of microgrids and battery swapping stations. Applied Energy 253, 113510.
Wu, H., Pang, G.K.-H., Choy, K.L., Lam, H.Y., 2017. A charging-scheme decision model for electric vehicle battery swapping station using varied population evolutionary algorithms. Applied Soft Computing 61, 905-920.
Xu, M., Yang, H., Wang, S., 2020. Mitigate the range anxiety: Siting battery charging stations for electric vehicle drivers. Transportation Research Part C: Emerging Technologies 114, 164-188.
Yan, J., Menghwar, M., Asghar, E., Panjwani, M.K., Liu, Y., 2019. Real-time energy management for a smart-community microgrid with battery swapping and renewables. Applied energy 238, 180-194.